Joint Special Interest Group meeting between euspen and ASPE
Dimensional Accuracy and Surface Finish in Additive Manufacturing,
KU Leuven, BE, October 2017
www.euspen.eu

Opto-mechanical modelling of an additive manufacturing laser scanning head including assembly defects

Kevin. Godineau[1], Sylvain. Lavernhe[1], Christophe. Tournier[1]

[1]*LURPA, ENS Cachan, Univ. Paris-Sud, Université Paris-Saclay, 94235 Cachan, France*

kevin.godineau@ens-paris-saclay.fr

Abstract
Additive manufacturing (AM) machines used in SLM or SLA are composed of galvanometric scanning system in order to focus and steer a laser beam to melt raw materials. A major problematic in these AM processes is to master the laser spot position which essentially depends on the machine geometry and the galvanometers angular positions. In literature, most of existing models make strong assumptions concerning the geometry of the laser scanning system. Moreover, the position of the laser spot is often obtained by interpolating a table of correspondence, experimentally determined, between the angular positions of the galvanometers and the cartesian coordinates in the working plane. All these approximations induce deviations of the laser spot compared to the desired position and affect machine performance. This article presents two kinematic models of the galvanometric laser scanning system in an AM machine: a nominal model of the system and a model with assembly defects consideration. These kinematic models, often used for machine tools and robots, are here applied to create a virtual AM machine. Thereby, the laser spot position can be simulated knowing the geometry of the machine, the possible assembly defects, and the orientation of the galvanometers. The second kinematic model is then used to extract the influence of assembly defects on the laser spot position. The work described in this paper allows us to highlight and quantify the theoretical impact of an assembly defect on the precision of the laser spot position in an AM machine.

Accuracy, Assembly, Defect, Geometric modelling

1. Introduction

In order to increase machine tools and robot performances, mathematical models have been developed to express the relationships between the work space (end-effector position) and the joint space (axes position). These models, which are now largely integrated within the NC controls, are enhanced by numerous behaviours (assembly defects, deformation of the structure due to cutting forces...). Thus, it's possible to take into account all these parameters to model the machine in order to remove as many undesirable behaviours as possible during machining.

The work presented in this article focuses on the kinematic modelling of SLM and SLA additive manufacturing machines. For these processes, opto-mechanical systems used to position precisely the laser spot on the material can be divided into two categories [1]: pre-objective laser scanning systems and post-objective laser scanning systems.

This article is only devoted to post-objective laser scanning systems. The laser beam passes through a focalization device and hits successively two rotary mirrors to be deviated towards the working plane to melt raw material. The rotary mirrors are actuated by two galvanometers and are used to precisely position the laser spot. In this system, the work space is defined by the laser spot position, and the joint space is defined by the galvanometers angular positions.

Well-known mathematical models establish the relationships between the laser spot position and the angular positions of the mirrors [2-6]. However, strong assumptions are made. For instance, the rotary axis and the reflection surface of the mirror are often mixed [2, 5, 6] which may simplify the geometry.

Furthermore, from a control point of view, to reduce the computation time, correspondence table is preferred to determine the position setpoints of the galvanometers from the laser positions. To ensure a high precision of the machines, the geometrical deviations of the laser on the working plane have to be compensated by the command [7]. But the identification of this compensation directly on the correspondence table can be a long and not optimal experimental process. It should be possible to take advantage of the continuous formulation of the geometry with defects to improve the building of the final correspondence table.

In this article, two kinematic models are proposed to model the actual behaviour of AM machines equipped with opto-mechanical systems. The novelty is to express directly the assembly errors of each subcomponent that make the laser spot position deviate from its nominal position. The aim of the study is to be able to visualize, to quantify and to understand the impact of these assembly defects onto the working plane.

The paper is then organized as following: Section 2 is dedicated to the nominal kinematic model of the full opto-mechanical system. Assembly defects are included inside the second model in section 3. Finally, in section 4, assembly defects and their influences on the working plane are analysed.

2. Nominal model

In order to define a mathematical formulation between joint space and work space, a nominal kinematic model is developed. This model describes the galvanometric scanning system operation. Parameters used in this model are named X, Y and Z for translations (A, B and C for rotations).

2.1. Assumptions and parameterization

Due to particles ejection and smoke production in selective laser melting context, two windows *w1* and *w2* are necessary to dissociate the production environment from the laser source environment. The nominal model of the system represented in figure 1 and figure 2 is submitted to the following assumptions:

1. The intersection of the laser beam and the work plane *p* is not influenced by the focalization device (Dynamic Focus Module or DFM). Therefore, only the laser beam positioning device is studied.
2. The origin of the laser source O_s is located at the centre of the DFM equivalent focus lens.
3. The laser beam hits the work plane perpendicularly in the following joint configuration: $(\theta_x, \theta_y) = (0,0)$. The intersection point is named O_p. For this configuration mirrors rotary axes are named *ax0* and *ay0*.
4. Flat surfaces (mirror surfaces, work plane, windows) are considered as perfect planes.
5. Windows thickness is constant and equal to e_v. Therefore, windows surfaces are parallel to each other.
6. Windows surfaces and work plane are also parallel to each other.
7. General geometrical optics properties are assumed. Therefore, the laser beam is modelled by a light ray.
8. Distance between the mirror rotary axis *ax* (*ay*) and the mirror reflection surface *mx* (*my*) is named e_m and is not equal to zero.

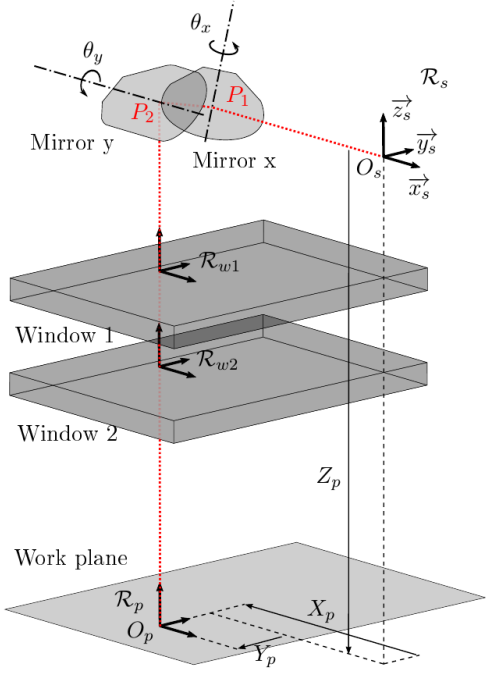

Figure 1. Nominal model

The nominal kinematic model is expressed considering the optical path and its successive transformations caused by each component. In order to establish more easily the kinematic model of the full device, the system is decomposed into local sub-models. Three sub-models are established. The first one, determine, whatever the system axis, the orientation of the light ray reflected by a mirror. The second sub-model gives the coordinates of the intersection point between the light ray and a flat surface. The last sub-model describes the deviation due to a window on light ray orientation and position. These three optical models render the forward kinematic model non-linear and do not allow us to use the work developed in the robotic system literature or machine tools literature.

The mathematical formulations are expressed with homogeneous formalism except for the three previous models. Transformation matrices are defined using extrinsic Tait-Bryan parameterization (xyz). Equation 1 represents the homogeneous transformation matrix to express a vector from the R_{ay0} frame into the R_s frame for the mirror y (figure 2 left):

$$T_{s/ay0} = \begin{pmatrix} 1 & 0 & 0 & 0 \\ 0 & \cos(A_{ay0}) & -\sin(A_{ay0}) & Y_{ay0} \\ 0 & \sin(A_{ay0}) & \cos(A_{ay0}) & Z_{ay0} \\ 0 & 0 & 0 & 1 \end{pmatrix} \quad (1)$$

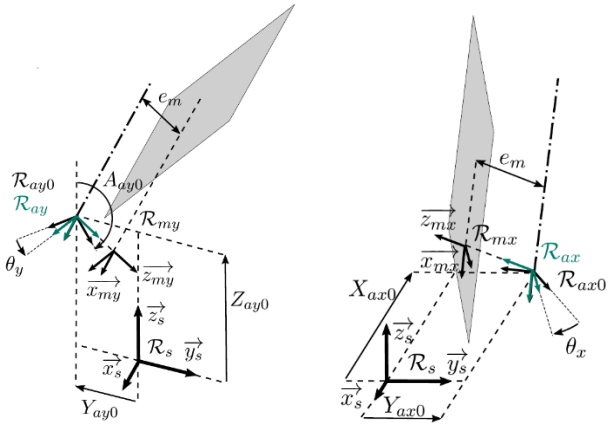

Figure 2. Mirror parameterization – mirror y (left), mirror x (right)

2.2. Forward Kinematic Model

The Forward Kinematic Model (FKM) of the system $(x, y) = h(\theta_x, \theta_y)$ is determined by following the light ray from the source to the work plane. By using the three sub-models and the transition matrix previously described, the FKM is obtained. Variables K_1, K_2 and K_3, defined by equations 2, 3 and 4 are used to reduce the FKM equations size in equations 5 and 6.

$$K_1 = \frac{e_m + Z_{ay0}\cos(A_{ay0} + \theta_y) - Y_{ay0}\sin(A_{ay0} + \theta_y)}{\cos(A_{ay0} - B_{ax0} + \theta_y)} \quad (2)$$

$$K_2 = Z_p + 2e_v - K_1\cos(B_{ax0}) \quad (3)$$

$$K_3 = \sqrt{\cos(2\theta_x)^2\cos(2\theta_y)^2 - 1 + \frac{n_2^2}{n_1^2}} \quad (4)$$

Many models of the literature are regrouped within this model. For example: the suppression of the windows ($e_v = 0$), the suppression of the mirror thickness ($e_m = 0$), and some assumptions about mirror positions allows this model

$$x = -X_p + X_{ax0} + \frac{e_m - Y_{ax0}\cos(-A_{ax0} + \theta_x)\sin(B_{ax0})}{\sin(-A_{ax0} + \theta_x)} - K_2\frac{\tan(2\theta_x)}{\cos(2\theta_y)} - K_1\tan(2\theta_x) + \frac{2e_v\sin(2\theta_x)}{K_3} \quad (5)$$

$$y = -Y_p - K_1\sin(B_{ax0}) - K_2\tan(2\theta_y) + \frac{2e_v\cos(2\theta_x)\sin(2\theta_y)}{K_3} \quad (6)$$

to represent the complex model described by [6]. Furthermore, as the nominal model takes into account many geometrical parameters, it allows us to model a wide variety of different two axis galvanometric laser scanning systems. Thanks to its low mathematical complexity, lots of real-time applications can embed such native equations.

Hence, this model represents a virtual machine. Coupled with the Inverse Kinematic Model (IKM), it allows us to simulate the opto-mechanical chain of an additive manufacturing process.

2.3. Inverse Kinematic Model

The inverse kinematic model $(\theta_x, \theta_y) = h^{-1}(x, y)$ is used to convert work space point coordinates (x, y) provided by the slicer to joint space setpoints (θ_x, θ_y). The Inverse Kinematic Model cannot be computed analytically considering the FKM equations and the non-linearities. Therefore, a Newton Raphson method is used to determine the solutions numerically. This method significantly increases the computation time compared to the FKM, which makes it impossible to be used for real time computations for scan speed interpolation. As mentioned previously, correspondence tables based on this kinematic model between the two spaces (joint space and work space) can be favorably used [7].

3. Model with regard to assembly defects

In this section, assembly defects are introduced inside the previous model in order to simulate the laser spot position knowing the geometry of the machine and the possible assembly defects.

3.1. List of assembly defects

There are numerous defects which disrupt the nominal operation of the laser scanner device: optical defects, surfaces geometrical defects, thermal defects which introduce deformations of all system parts, dynamic defects... The rest of the article focuses on one of the major issues: the assembly defects, i.e., the non-nominal assembly of sub-components considering that each one is without defect.

The previous model assumptions remain valid except the third assumption and the sixth assumption mentioned above. Due to the parameterization of the nominal model, thirty assembly defects that significantly influence the laser spot position have been identified. Those assembly defects are collected in table 1. Each defect is noted δ, the indices *x*, *y* and *z* (or *a*, *b* and *c*) correspond to the position defects along the axes *x*, *y* and *z* (or rotation defects around the axes *x*, *y* and *z*).

Table 1. List of all assembly defects included in the kinematic models.

	x	y	z	a	b	c
Laser source		δ_{y_s}	δ_{z_s}		δ_{b_s}	δ_{c_s}
Rotary axis x		$\delta_{y_{ax}}$	$\delta_{z_{ax}}$	$\delta_{a_{ax}}$	$\delta_{b_{ax}}$	$\delta_{c_{ax}}$
Mirror x			$\delta_{z_{mx}}$	$\delta_{a_{mx}}$	$\delta_{b_{mx}}$	
Rotary axis y		$\delta_{y_{ay}}$	$\delta_{z_{ay}}$	$\delta_{a_{ay}}$	$\delta_{b_{ay}}$	$\delta_{c_{ay}}$
Mirror y			$\delta_{z_{my}}$	$\delta_{a_{my}}$	$\delta_{b_{my}}$	
Windows 1				$\delta_{a_{w1}}$	$\delta_{b_{w1}}$	
Windows 2				$\delta_{a_{w2}}$	$\delta_{b_{w2}}$	
Work plane	δ_{x_p}	δ_{y_p}	δ_{z_p}	δ_{a_p}	δ_{b_p}	δ_{c_p}

3.2. Integration of assembly defects

The modelling of the thirty assembly defects inside the opto-mechanical chain is represented in figure 3. Those defects are integrated in the nominal model by adding new non-linearized homogeneous transformation matrices. For example, in the nominal model, in order to pass from the mirror frame to the source frame, three transformation matrices are necessary ($T_{ax/m}$, $T_{ax0/ax}$, $T_{s/ax0}$). For the model with defects, six transformation matrices are now necessary ($T_{m/mdef}$, $T_{axdef/m}$, $T_{ax/axdef}$, $T_{ax0/ax}$, $T_{s/ax0}$, $T_{sdef/s}$).

This new FKM with assembly defects consideration $(x, y) = h_{\boldsymbol{\delta}}(\delta_{y_s}, \dots, \delta_{c_p}, \theta_x, \theta_y)$ allows to simulate a greater number of possible behaviors of the system to represent the actual one. Moreover, the assembly defects inserted in the final model are not linearized, therefore it is possible to completely modify the geometry of the system by interpreting geometric defects as new geometrical parameters.

The IKM with defects is also solved with a Newton Raphson method. However, increasing the number of variables increases the mathematical complexity of the model leading to longer computation time of the jacobian matrices.

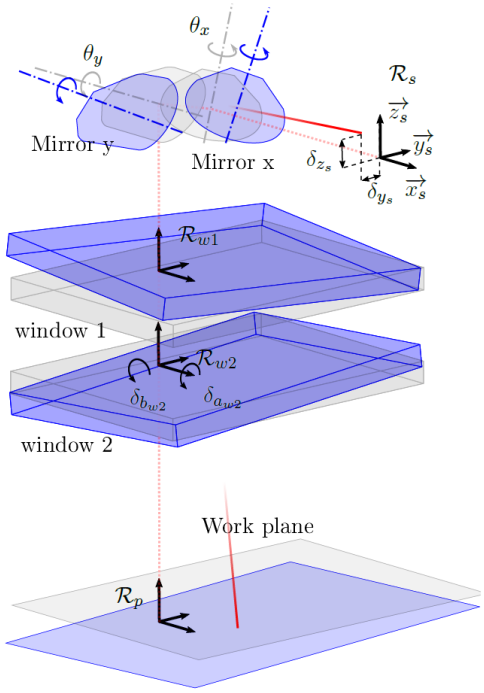

Figure 3. Representation of assembly defects in the model

4. Influence of assembly defects

In this section, the two previous models are used to visualize and characterize the influence of assembly defects on the laser spot position in the working plane.

4.1. Visualization of assembly defects

The subtraction between the second model (model with all assembly defects) and the first model (nominal assembly model) allows us to quantify the theoretical impact of each assembly defect on the laser spot position (cf. equation 7). Indeed, by setting successively all defects parameters to zero except δ_i which is analysed in the function h_{δ_i}, its influence I_{δ_i} is directly obtained for all mirrors' positions.

$$I_{\delta_i}(\theta_x, \theta_y) = h_{\delta_i}(0, \dots, 0, \delta_i, 0, \dots, 0, \theta_x, \theta_y) - h(\theta_x, \theta_y) \quad (7)$$

Figure 4 represents $I_{\delta_{y_s}}(\theta_x, \theta_y)$, the displacement of the laser spot for all joint configurations when a unitary assembly

defect δ_{y_s} = 1 *mm* is introduced. Arrows indicate the direction of the deviation and colors indicate its magnitude.

The displacement of the laser spot position induced by the laser source assembly defect δ_{y_s} can be divided into two components. The first one, represents the global displacement of the laser spot positions. This displacement is called linear displacement because it is due to the O_p point displacement for the joint configuration $(\theta_x, \theta_y) = (0, 0)$, when the assembly defect is added. In figure 4 this global linear displacement is equal to 1 *mm*. The second component of the displacement represents the non-linearity of the two mirrors. The shape of this displacement is mainly due to the position where the laser spot hits the mirror x compared to the position of the mirror rotary axis x. This displacement, called non-linear displacement, is about 0.1 *mm* in figure 4.

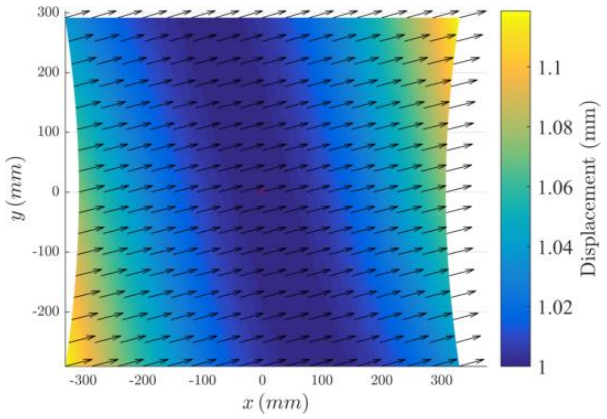

Figure 4. Impact of the assembly defect ($\delta_{y_s} = 1\ mm$) on the laser spot position.

4.2 Impact and characterization of each assembly defect

Figure 5 gathers the deviation magnitudes caused on the spot position by a unitary influence ($\delta_? = 1\ mm$) for the eleven positioning defects. Each assembly defect is represented by a bar, the linear component of the displacement due to assembly defects is represented by the first value of the colorbar (white area) while the non-linear component is represented by the colorbar itself (blue to yellow area). The first bar corresponds to the assembly defect δ_{y_s} represented in figure 4.

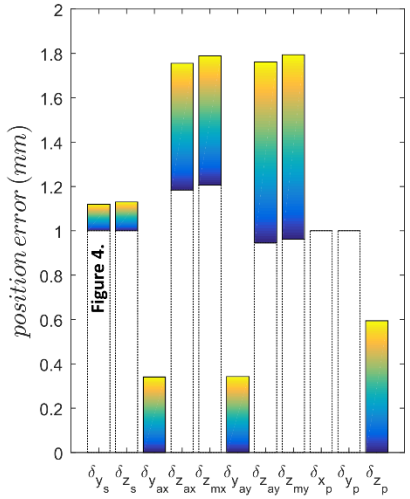

Figure 5. Macroscopic characterization of each position assembly defect influence.

Figure 5 shows that δ_{x_p} and δ_{y_p} have only the linear displacement component. The assembly defects $\delta_{y_{ax}}$, $\delta_{y_{ay}}$ *and* δ_{z_p} are only composed by the non-linear component of the displacement. The nineteen orientation defects can also be represented in a similar figure. This figure, not represented in this article, would show that windows orientation defects have a negligible impact compared to other defects (relative influence equal to 1000). In general terms, the more the spot laser is distant to the origin O_p, the larger are the defects influences on the laser spot position and so on the machine precision.

Using the developed models, a virtual machine is created to quantify the displacement error of the laser spot. Figure 6 represents this error for an AM machine which the assembly defects include in Table 2. Assembly defects are randomly generated between ± 0.1 *mm* for position defects and ± 0.1 *mrad* for orientation defects.

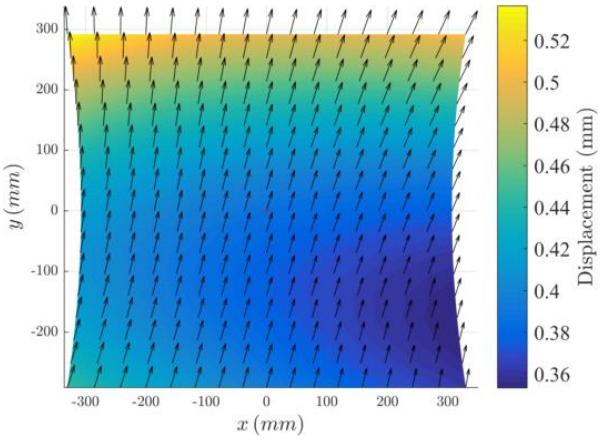

Figure 6. Impact of 30 different assembly defects (cf. Table 2) on the laser spot position.

Table 2. Values of assembly defects included in the kinematic model which generates the Figure 6.

defect	*mrad*
δ_{b_s}	-0.0693
δ_{c_s}	-0.0654
$\delta_{a_{ax}}$	0.0302
$\delta_{b_{ax}}$	0.0635
$\delta_{c_{ax}}$	0.0533
$\delta_{a_{mx}}$	-0.0621
$\delta_{b_{mx}}$	0.0293
$\delta_{a_{ay}}$	0.0277
$\delta_{b_{ay}}$	0.0184
$\delta_{c_{ay}}$	-0.0349
$\delta_{a_{my}}$	-0.0754
$\delta_{b_{my}}$	0.0472
$\delta_{a_{w1}}$	-0.0687
$\delta_{b_{w1}}$	-0.0131
$\delta_{a_{w2}}$	0.0665
$\delta_{b_{w2}}$	-0.0280
δ_{a_p}	-0.0736
δ_{b_p}	0.0399
δ_{c_p}	-0.0028

defect	*mm*
δ_{y_s}	-0.0633
δ_{z_s}	-0.0846
$\delta_{y_{ax}}$	-0.0398
$\delta_{z_{ax}}$	-0.0232
$\delta_{z_{mx}}$	-0.0252
$\delta_{y_{ay}}$	-0.0993
$\delta_{z_{ay}}$	-0.0434
$\delta_{z_{my}}$	0
δ_{x_p}	-0.0848
δ_{y_p}	0.0114
δ_{z_p}	-0.0452

5. Conclusion and perspectives

In order to study the impact of assembly defects on the laser spot position, two models have been created. The first model represents the nominal system. The second model introduces thirty assembly defects to represent more precisely the behavior of a real machine. These two models allow to highlight and quantify the theoretical impact of an assembly defect on the precision of the laser spot position in an AM machine.

One of the major perspectives of this study consists in identifying the values of the assembly defects from experimental measurements of the laser spot position. Hence, the use of these models would save a lot of time during the calibration phase of the AM machine.

References

[1] Ehrmann J S, "Optics for vector scanning", Beam Deflection and Scanning Technologies, *SPIE* vol. **1454** pp. 245-255, 1991.

[2] Cui S, Zhu X, Wang W et Xie Y, "Calibration of a laser galvanometric scanning system by adapting a camera model" *Appl. Opt.,* vol. **48**, pp. 2632-2637, 2009.

[3] Eberle G, Dold C and Wegener K, "Building a vector model representation of a two-axis laser scanhead using numerical analysis for simulation purposes" *IJMIC,* vol. **20**, pp. 199-207, 2013.

[4] Li Y, "Beam deflection and scanning by two-mirror and two-axis systems of different architectures: a unified approach" *Appl. Opt.,* vol. **47**, pp. 5976-5985, 2008.

[5] Xie J, Huang S, Duan Z, Shi Y and Wen S, "Correction of the image distortion for laser galvanometric scanning system" *Optics & Laser Technology,* vol. **37**, pp. 305-311, 2005.

[6] Manakov A, Seidel H-P and Ihrke I, "A Mathematical Model and Calibration Procedure for Galvanometric Laser Scanning Systems" 2011.

[7] Delgado M A O et Lasagni A F, "Reducing field distortion for galvanometer scanning system using a vision system" *Optics and Lasers in Engineering,* vol. **86**, pp. 106-114, 2016.